



# Fluorinated electrolyte for 4.5 V Li(Ni<sub>0.4</sub>Mn<sub>0.4</sub>Co<sub>0.2</sub>)O<sub>2</sub>/graphite Li-ion cells



Jian Xia<sup>a</sup>, M. Nie<sup>a</sup>, J.C. Burns<sup>b</sup>, A. Xiao<sup>c</sup>, W.M. Lamanna<sup>c</sup>, J.R. Dahn<sup>a,\*</sup>

<sup>a</sup> Dept. of Physics and Atmospheric Science, Dalhousie University, Halifax, NS, Canada B3H3J5

<sup>b</sup> Novonix Corp., 1 Research Drive, Dartmouth, NS, Canada

<sup>c</sup> Electronic Materials Solutions Division, 3M Co., 3M Center, St. Paul, MN, USA

## HIGHLIGHTS

- Fluorinated electrolyte leads to better tolerance of Li-ion cells to high potentials.
- Impedance increase at positive electrodes is mitigated using fluorinated electrolyte.
- However, fluorinated electrolyte leads to high impedance at the negative electrode.
- A wide variety of fluorinated solvents need to be explored with the methods described.

## ARTICLE INFO

### Article history:

Received 23 October 2015

Received in revised form

15 December 2015

Accepted 28 December 2015

Available online 9 January 2016

### Keywords:

Fluorinated electrolytes

High voltage Li-ion cells

Impedance growth

Gas generation

Battery lifetime

High precision coulometry

## ABSTRACT

A fluorinated electrolyte mixture, containing 1 M LiPF<sub>6</sub>/fluoroethylene carbonate:bis (2,2,2-trifluoroethyl) carbonate (1:1 w:w) with prop-1-ene-1,3-sultone as an electrolyte additive exhibited promising cycling and storage performance in Li(Ni<sub>0.4</sub>Mn<sub>0.4</sub>Co<sub>0.2</sub>)O<sub>2</sub>/graphite pouch type Li-ion cells tested to 4.5 V. The prop-1-ene-1,3-sultone additive was added to help control gas evolution in the fluorinated electrolyte cells, which was improved but still problematic even with the additive. Cells with the fluorinated electrolyte demonstrated higher impedance in early cycles compared to cells with carbonate solvents and state of the art additives. Symmetric cells were used to show this high impedance originated at the negative electrode/electrolyte interface. Nevertheless, in charge–discharge cycling tests to 4.5 V, cells with the fluorinated electrolyte and 1, 2 or 3% prop-1-ene-1,3-sultone additive, outperformed all non-fluorinated electrolytes with all additives tested. With further work, these, or other fluorinated carbonates, coupled with appropriate additives, may represent a viable path to NMC/graphite cells that can operate to 4.5 V and above.

© 2015 Elsevier B.V. All rights reserved.

## 1. Introduction

Li-ion batteries with higher power and energy density are desired for smart mobile devices, electric vehicles and grid energy storage [1,2]. Developing novel high voltage cathode materials or simply increasing the cut-off voltage of the traditional cathode materials could improve power or energy density [3–7]. However, there is no commercial electrolyte available for these high voltage cells since state-of-the-art electrolytes containing organic carbonates and typical salts are prone to decompose at high potentials [8,9]. The development of new solvents with a broad voltage

window that stabilize the positive electrode/electrolyte interphase remains an ongoing task.

Fluorinated organic carbonates have higher oxidation stability, lower flammability as well as lower melting point compared with their corresponding non-fluorinated carbonates [10,11]. These fluorinated organic compounds have been studied as co-solvents or electrolyte additives to improve the safety characteristics and cycle performance of Li-ion cells. For example, Cresce et al. [12] reported that the fluorinated phosphate ester structure was able to stabilize carbonate electrolytes on the surface of 5 V class positive electrodes. Smart et al. [13] synthesized a series of fluorinated linear carbonates and incorporated them with traditional cyclic and linear aliphatic carbonates to improve the low temperature performance of MCMB/Li and LiNiCoO<sub>2</sub>/MCMB cells. Chen and Holstein et al. [14] showed LiNi<sub>0.5</sub>Mn<sub>1.5</sub>O<sub>4</sub> (LNMO)/Li<sub>4</sub>Ti<sub>5</sub>O<sub>12</sub> coin type cells containing

\* Corresponding author.

E-mail address: [jeff.dahn@dal.ca](mailto:jeff.dahn@dal.ca) (J.R. Dahn).

a solvent mixture comprising 2,2,-difluoroethyl acetate and EC could cycle 300 times using a current corresponding to C/2 at 55 °C with a capacity retention of 44%. Zhang and Amine et al. [15] investigated a series of fluorinated carbonates in LNMO/Li and LNMO/Li<sub>4</sub>Ti<sub>5</sub>O<sub>12</sub> coin-type cells and found these all-fluorinated electrolytes showed higher lithium ion conduction and superior anodic stability at elevated temperatures compared to EC/EMC-based electrolytes. However, when cycled in LNMO/graphite chemistry, cells containing these all-fluorinated electrolytes lost more than 50% of their initial capacity after only 100 cycles at C/3 and 3.5–4.9 V at 55 °C [16]. Even when some fluorinated additives were incorporated, the capacity retention was not greatly improved [16]. The coulombic efficiencies of cells containing the all-fluorinated electrolytes described by Zhang and Amine et al. was only 92% under the conditions in that report and, therefore, it is not surprising that cells with these all-fluorinated electrolytes showed poor capacity retention. The same group also found that when fluorinated cyclic carbonate (F-AEC) was substituted by fluoroethylene carbonate (FEC) [17] or when a lithium reservoir was added [18], the cycling performance in LNMO/graphite coin type cells was then improved.

Li[(Ni<sub>1/2</sub>Mn<sub>1/2</sub>)<sub>1-x</sub>Co<sub>x</sub>]O<sub>2</sub> is of particular interest as a positive electrode material because reducing the Co content reduces the materials cost. Li[(Ni<sub>1/2</sub>Mn<sub>1/2</sub>)<sub>1-x</sub>Co<sub>x</sub>]O<sub>2</sub> offers improved thermal and safety properties compared to LiCoO<sub>2</sub> and higher specific capacity if the charge cutoff can be increased above 4.5 V [19,20]. Li(Ni<sub>0.4</sub>Mn<sub>0.4</sub>Co<sub>0.2</sub>)O<sub>2</sub> (NMC442) can be operated up to 4.7 V without structural damage [21]. The voltage (V) vs capacity (Q) curve of NMC442 is relatively linear between 4.1 and 4.7 V so that the dependence of the coulombic efficiency and other properties on potential can be measured as the upper cut-off potential is sequentially increased.

Aiken et al. [22] and Self et al. [23] showed that a second gas evolution step was observed in NMC442/graphite pouch cells during the formation cycle above 4.3 V due to the electrolyte oxidation at the positive electrode. Nelson et al. [24] and Ma et al. [25] showed that the impedance of NMC442/graphite pouch cells continues to grow during long term cycling when cells were charged to 4.4 V or above, although this can be mitigated somewhat using appropriate electrolyte additives. Using symmetric cell studies, Petibon et al. [26] showed that the majority of this impedance growth occurs at the positive electrode. This suggests that electrolyte/positive electrode reactions - electrolyte oxidation - are the major problem that causes cell failure for NMC442/graphite cells charged to high potentials (>4.4 V).

Here, the fluoroethylene carbonate (FEC) - bis(2,2,2-trifluoroethyl) carbonate (TFEC) solvent system with different amounts of the additive prop-1-ene-1,3-sultone (PES) was studied in NMC442/graphite pouch type Li-ion cells. Fig. 1a shows the chemical structures of FEC, TFEC and PES. Experiments were made using Ultra High Precision Coulometry (UHPC) [27], a precision storage system [28], an *in-situ* gas evolution apparatus [29], long term cycling, electrochemical impedance spectroscopy (EIS) and EIS measured automatically during long term cycling [24]. Gas evolution during formation and cycling, coulombic efficiency, charge endpoint capacity slippage during cycling and EIS spectra before and after cycling were examined and compared. Long-term cycling results compared the cycling performance of NMC442/graphite cells with FEC:TFEC:PES electrolyte (no EC) to cells with 1 M LiPF<sub>6</sub> EC:EMC (3:7 wt.%) and the additive set, 2% PES + 1% MMDS + 1% TTSPi.

## 2. Experimental

1 M LiPF<sub>6</sub> EC:EMC (3:7 wt.% ratio, BASF, 99.99%) was used as the

control electrolyte. The TFEC was obtained from HSC Corporation (Jiangsu, China, 99.80 wt.%) while the FEC was from BASF (99.94%). 1 M LiPF<sub>6</sub> FEC:TFEC (1:1 wt.% ratio) was used as the studied electrolyte. To the studied electrolyte, the additive Prop-1-ene-1,3-sultone (PES, Lianchuang Medicinal Chemistry Co., Ltd., China, 98.20%) was added at 1, 2, 3, 5 and 8% by weight. 2% PES + 1% MMDS (or DTD) + 1% TTSPi (PES 211) in EC:EMC (3:7 wt.%) electrolyte was used for comparison in the long-term cycling tests. The details of PES211 additive combinations have been reported in Ref. [25].

The pouch cells employed in this study were all Li[Ni<sub>0.4</sub>Mn<sub>0.4</sub>Co<sub>0.2</sub>]O<sub>2</sub> (NMC442)/graphite cells with a capacity of 245 mAh balanced for 4.7 V operation. SEM images of the NMC442 and graphite electrodes are shown in Ref. [30]. The cells were produced by Li-Fun Technology (Xinma Industry Zone, Golden Dragon Road, Tianyuan District, Zhuzhou City, Hunan Province, PRC, 412000). The pouch cells were vacuum sealed without electrolyte in China and then shipped to our laboratory in Canada. Before filling with electrolyte, the cells were cut just below the heat seal and dried at 80 °C under vacuum for 14 h to remove any residual water. Then the cells were transferred immediately to an argon-filled glove box for filling and vacuum sealing. The NMC442/graphite pouch cells were filled with 0.75 mL of electrolyte (0.90 g for control electrolyte and 1.17 g for FEC:TFEC electrolyte. The density of FEC:TFEC electrolyte is 1.56 g/mL compared to 1.21 g/mL for control electrolyte). After filling, cells were vacuum-sealed with a compact vacuum sealer (MSK-115A, MTI Corp.). First, cells were placed in a temperature box at 40.0 °C where they were held at 1.5 V for 24 h, to allow for the completion of wetting. Then, cells were charged at 12 mA (C/20) to 3.5 V. This step is called formation step 1. After formation step 1, cells were transferred into the glove box, cut open to release any gas generated and vacuum sealed again. These cells were then charged from 3.5 V at 12 mA (C/20) to 4.5 V. This step is called formation step 2. After formation step 2, the cells were transferred into the glove box, cut open to release gas generated and then vacuum sealed again. These degassing voltages were selected based on the *in-situ* gas evolution experiments, to be described below, that show most of the gas evolves in the formation step at voltages below 3.5 V and above 4.3 V [22]. After the two degassing processes, cells were then discharged to 3.8 V where impedance spectra were measured.

The cycling/storage procedure was carried out using the Ultra High Precision Charger (UHPC) at Dalhousie University [27]. Testing was between 2.8 and 4.4 V at 40. ± 0.1 °C. Cells were first charged to 4.400 V using currents corresponding to C/10, stored open circuit at 4.400 V for 20.00 h and then discharged to 2.800 V using currents corresponding to C/10. This process was repeated on the UHPC for 15 cycles where comparisons were made. The cycling/storage procedure [30] was designed so that the cells were exposed to higher potentials for significant fractions of their testing time. For storage experiments, cells were first discharged to 2.8 V and charged to 4.5 V two times. Then the cells were held at 4.5 V until the measured current decreased to 0.0025 C. A Maccor series 4000 cyler was used for the preparation of the cells prior to storage. After the pre-cycling process, cells were carefully moved to the storage system which monitored their open circuit voltage every 6 h for a total storage time of 500 h at 40. °C [31].

Both *in-situ* (dynamic) and *ex-situ* (static) gas measurements were used to measure gas evolution during formation and during cycling [27]. Both measurements were made using Archimedes' principle with cells suspended from a balance while submerged in liquid. The changes in the weight of the cell suspended in fluid, before, during and after testing are directly related to the volume changes by the change in the buoyant force. The change in mass of a cell, Δm, suspended in a fluid of density, ρ, is related to the change

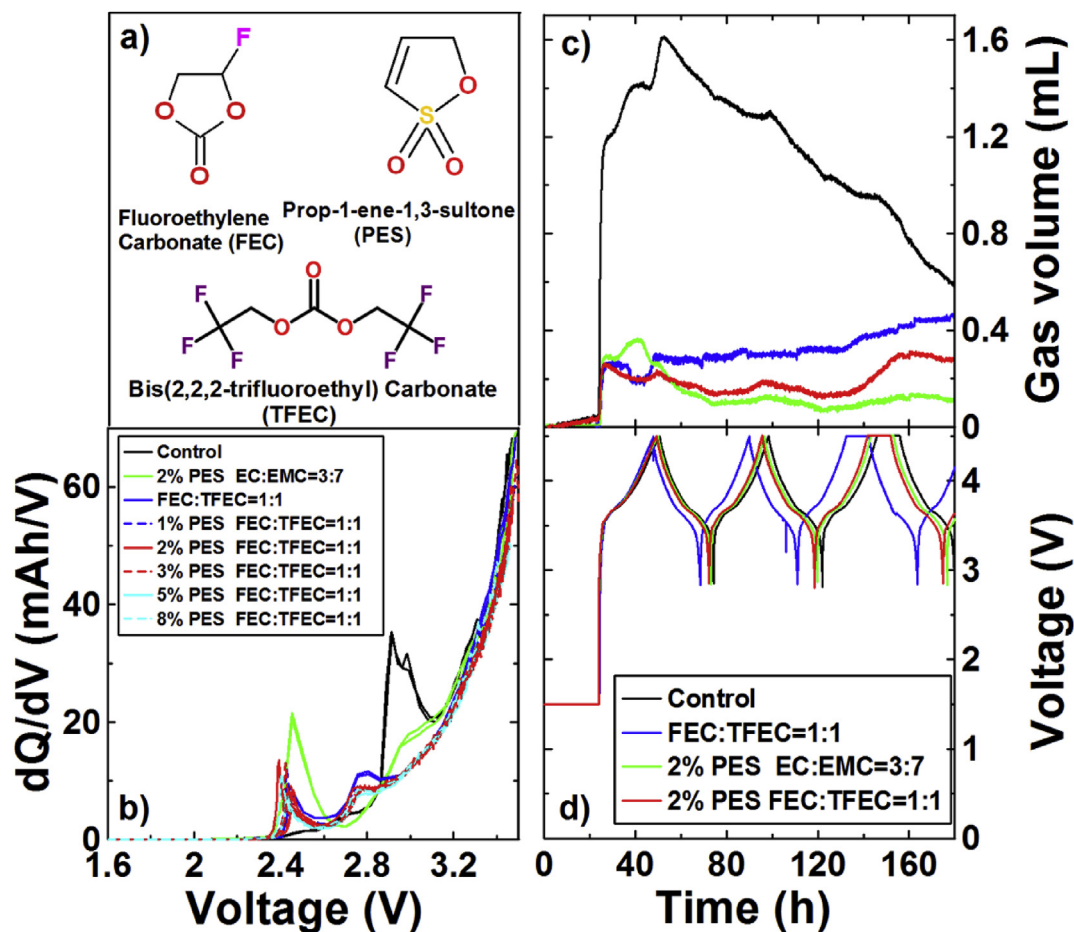


**Fig. 1.** (a) Chemical structures of FEC, TFEC and PES; (b) Differential capacity ( $dQ/dV$ ) versus potential (V) during formation step 1 for the 240 mAh NMC442/graphite pouch cells with different amounts of PES in FEC:TFEC electrolyte; (c) Gas volume versus time measured using the Archimedes' *in-situ* gas analyzer [22] during the first ~180 h (3 cycles); (d) Cell potential versus time during the *in situ* gas measurement. Panels c) and d) share a common x-axis.

in cell volume,  $\Delta v$ , by

$$\Delta v = -\Delta m/\rho \quad (1)$$

*Ex-situ* measurements were made by suspending pouch cells from a fine wire “hook” attached under a Shimadzu balance (AUW200D). The pouch cells were immersed in a beaker of de-ionized “nanopure” water (18 M $\Omega$ ) that was at  $20 \pm 1$  °C for measurement. Before weighing, all cells were charged or discharged to 3.80 V. *In-situ* measurements were made using the apparatus and procedure described in Ref. [29]. This apparatus can measure the gas evolution in up to six pouch cells simultaneously during operation. During the *in-situ* measurements, the cells were suspended in silicone vacuum pump oil and their mass was measured using sensitive strain gauges (or load cells) while they were charged and discharged. All *in-situ* gas volume measurements were made in a temperature box at  $40. \pm 0.1$  °C. During these measurements, cells were charged and discharged without degassing.

Electrochemical impedance spectroscopy (EIS) measurements were conducted on NMC111/graphite pouch cells after formation and also after cycling on the UHPC. Cells were charged or discharged to 3.80 V before they were moved to a  $10. \pm 0.1$  °C temperature box. Alternating current (AC) impedance spectra were collected with ten points per decade from 100 kHz to 10 mHz with a signal amplitude of 10 mV at  $10. \pm 0.1$  °C. A Biologic VMP-3 was used to collect these data.

Symmetric cells were made from electrodes obtained from some of these pouch cells after cycling. Symmetric cells were made by the procedures described Petibon et al. [32]. The pouch cells were charged or discharged to 3.80 V (approx. 50% state of charge) before they were opened in an argon-filled glove box. Six coin-cell size (1.54 cm<sup>2</sup>) positive electrodes and six coin-cell size (1.54 cm<sup>2</sup>) negative electrodes were cut from the pouch cells electrodes with a precision punch. Two negative symmetric coin cells, two positive symmetric coin cells and two full coin cells were reassembled using one polypropylene blown microfiber separator (BMF – available from 3 M Co., 0.275 mm thickness, 3.2 mg/cm<sup>2</sup>). The electrolyte used for the symmetric cells was the same as that used in the parent pouch cell. A positive electrode symmetric cell was constructed using two positive electrodes, and a negative electrode symmetric cell was constructed using two negative electrodes. A full coin cell was constructed using one positive electrode and one negative electrode.

Some cells were tested on an automated EIS/cycling system extremely aggressively to really push the limits of the electrolyte [33,34]. The cells were charged and discharged at 80 mA current between 2.8 and 4.5 V and held at 4.5 V for 24 h at  $40. \pm 0.1$  °C before discharging again on a Neware cyler. Automated impedance spectroscopy measurements were made after every three charge-hold-discharge cycles using a frequency response analyzer (FRA)/cyler system built at Dalhousie University. During FRA measurements, the cells were charged and discharged at 12 mA and

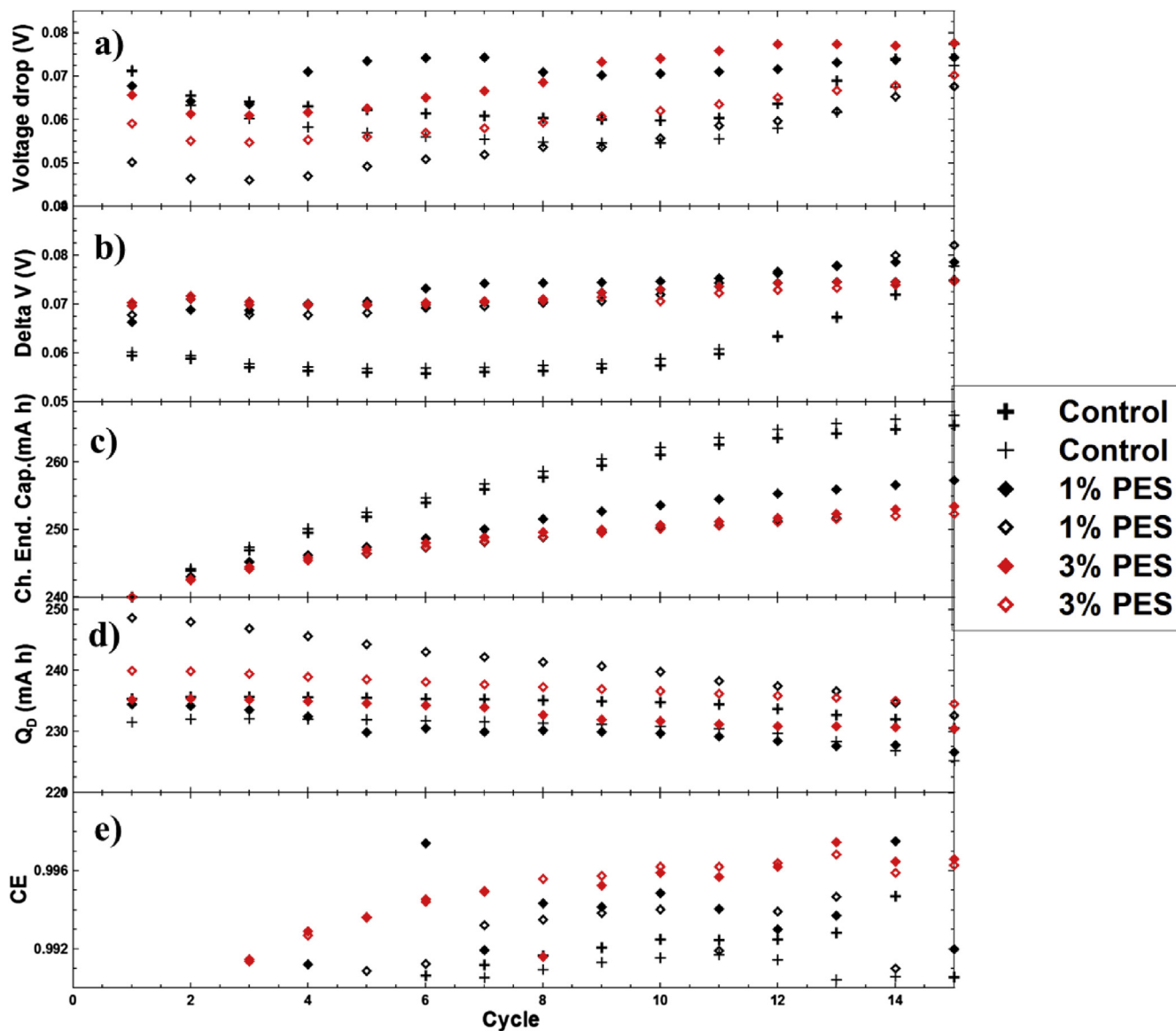


Fig. 2. Cycle/store data collected on the UHPC including: (a)  $V_{\text{drop}}$ , (b)  $\Delta V$ , (c) the charge endpoint capacity, (d) the discharge capacity and (e) the coulombic efficiency (CE). All data are plotted versus cycle number for NMC442/graphite pouch cells with control or different amounts of PES in FEC:TFEC electrolyte.

AC impedance spectra were collected every 0.1 V.

For long-term cycling, all cells were continuously cycled between 2.8 V and 4.5 V at  $40. \pm 0.5$  °C, using currents corresponding to C/2.4 (100 mA). A low rate C/10 cycle was included every 50 cycles to estimate what fraction of the capacity loss was due to impedance growth during the high rate cycling. The long-term cycling cells were the same cells used for the UHPC cycle/store experiments and long term cycling commenced after the UHPC tests completed. The cells were degassed after the UHPC cycling, before long term cycling commenced. During the long term cycling, all of the cells were cycled with clamps in place to maintain pressure on the electrode stack.

### 3. Results and discussion

Fig. 1b shows the differential capacity ( $dQ/dV$ ) vs. V curves of NMC442/graphite pouch cells with different amounts of PES during formation step 1. From the  $dQ/dV$  vs. V curves, one can determine at which potential the additives or solvents initially react with the

graphite electrode. The control cells showed a pronounced peak at 2.9 V which corresponds to a potential of  $\sim 0.75$  V vs.  $\text{Li/Li}^+$ . When 2% PES was added to the control electrolyte, the peak shifted to a lower potential of  $\sim 2.45$  V which corresponds to about 1.2 V vs.  $\text{Li/Li}^+$ . The  $dQ/dV$  vs. V curves of the cells with FEC:TFEC have two main peaks at cell potentials of about 2.4 V (1.25 V vs.  $\text{Li/Li}^+$ ) and about 2.7 V (0.95 V vs.  $\text{Li/Li}^+$ ). Fig. 1b shows that when PES was added in the FEC:TFEC system, both peaks shifted to a slightly higher potential. Compared with 2% PES in EC:EMC electrolyte, the addition of PES to FEC:TFEC electrolyte does not show an obvious peak.

To determine which electrolyte component reacts first on the negative electrode, some of the cells were formed with PES, FEC or TFEC as electrolyte additives in EC:EMC electrolyte (Fig. S1). Fig. S1a shows that both PES and FEC have a reduction peak at  $\sim 2.4$  V vs.  $\text{Li/Li}^+$  while TFEC has almost no impact in EC:EMC electrolyte during formation (just like control). Fig. S1b show the  $dQ/dV$  vs. V curve with different ratios of FEC:TFEC (without PES) during formation. Fig. S1b shows that an increasing ratio of FEC leads to a

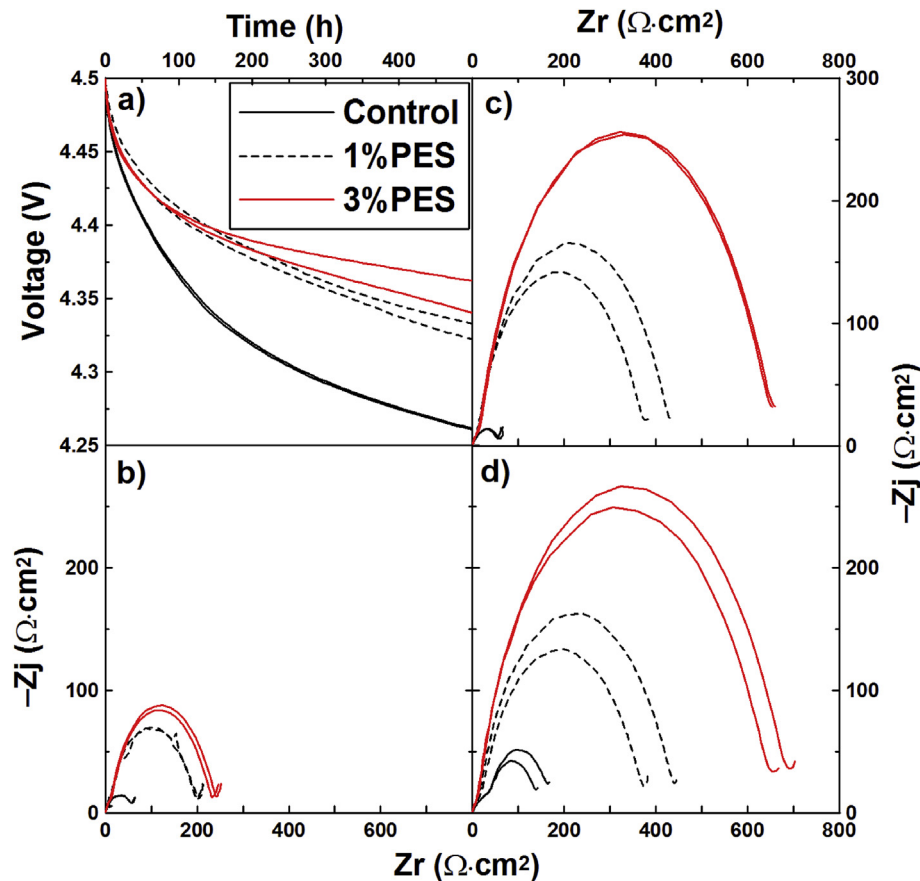


Fig. 3. (a) Open circuit potential versus time of NMC442/graphite pouch cells charged to 4.5 V with different amounts of PES in FEC:TFEC electrolyte stored at  $40 \pm 0.1$  °C; Impedance spectra at measured at 3.8 V and at  $10 \pm 0.1$  °C of NMC442/graphite pouch cells with different concentrations of PES in FEC:TFEC electrolyte: (b) after formation at  $40 \pm 0.1$  °C, (c) after UHPC cycle/store at  $40 \pm 0.1$  °C, (d) after storage at 4.5 V and  $40 \pm 0.1$  °C for 500 h.

lower reduction potential during formation. Based on the results in Fig. S1, it is very likely that FEC and PES initially react at the negative electrode while TFEC does not.

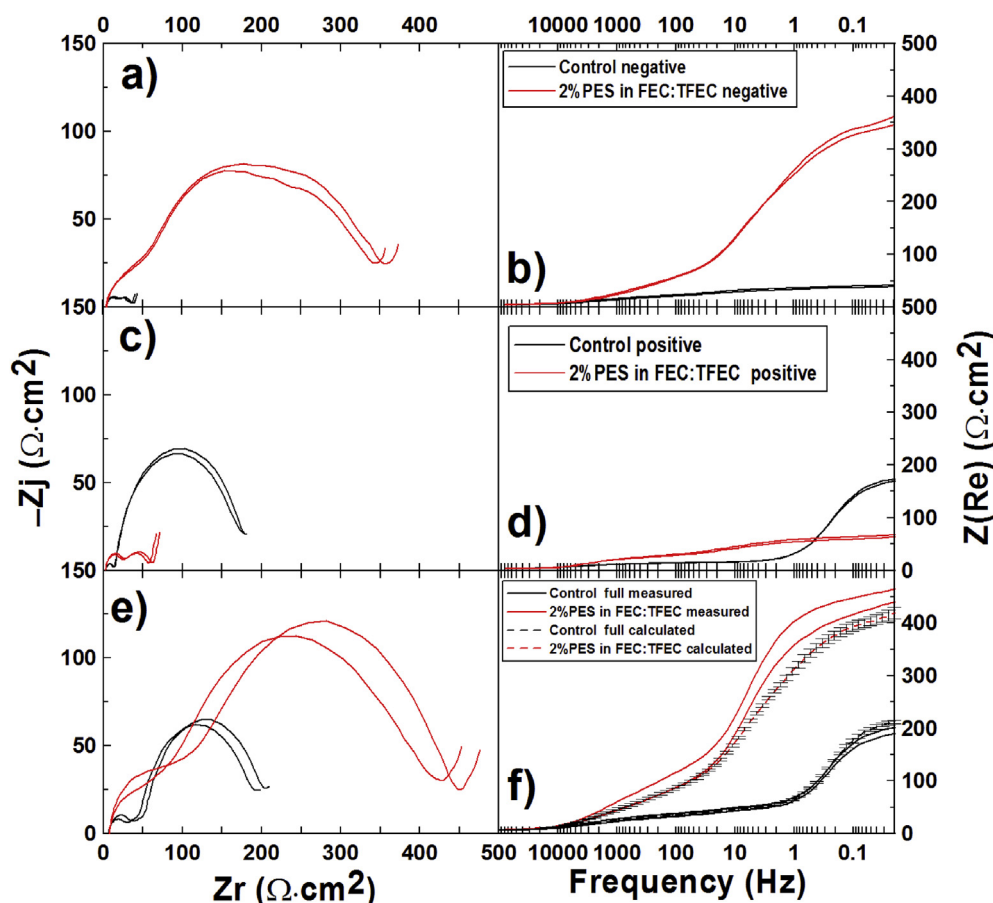
Fig. 1c shows the *in-situ* gas volume versus time during two charge–discharge cycles and one charge–hold cycle for the NMC442/graphite pouch cells with EC:EMC-based or FEC:TFEC-based electrolytes. Fig. 1d shows the cell voltage versus time for the same pouch cells measured during *in-situ* gas measurements. Fig. 1c shows that all cells have an initial gas evolution peak, mainly between 1.5 and 3.5 V. After the first gas evolution peak, the control cell continues to produce gas when charged to higher voltage, while the other three cells, which contain 1 M LiPF<sub>6</sub> in FEC:TFEC, 1 M LiPF<sub>6</sub> in 2% PES in EC:EMC and 1 M LiPF<sub>6</sub> in 2% PES in FEC:TFEC electrolyte, show gas consumption, mainly between 3.5 V and 4.3 V. When the cell voltage rises above 4.3 V, all cells show a second gas evolution peak, which is mainly due to electrolyte oxidation at the positive electrode [23]. Fig. 1c shows adding PES to both EC:EMC and FEC:TFEC greatly decreases the gas evolution in the high potential gas step, which agrees well with previous results on the effects of PES [35,36].

Fig. 2 shows the cycling/storage data collected using the UHPC for NMC442/graphite pouch cells with control electrolyte and with different amounts of PES in FEC:TFEC 1:1 electrolyte at  $40 \pm 0.1$  °C. From top to bottom, the five panels in Fig. 2 show: the voltage drop during the 20 h storage period at the beginning of each cycle,  $V_{\text{drop}}$ ; the difference between the average cell potential during charge and the average cell potential during discharge,  $\Delta V$ ; the charge endpoint capacity; the discharge capacity; and the coulombic

efficiency, all plotted versus cycle number. The differences in  $V_{\text{drop}}$  from cell to cell are caused by differences in the rate of electrolyte oxidation at the positive electrode surface and also by differences in DC cell resistance which affect the rapid potential change when the cells switch from charge to open circuit. Differences in  $\Delta V$  are caused by differences in cell polarization during cycling and smaller values of  $\Delta V$  generally indicate lower DC resistance [37]. Therefore some degree of correlation is expected between  $V_{\text{drop}}$  and  $\Delta V$  in Fig. 2a and b.

Fig. 2a and b shows that  $V_{\text{drop}}$  and  $\Delta V$  for control cells rises rapidly during the last five cycles due to impedance growth. By contrast, cells with 1% PES or 3% PES in FEC:TFEC do not show this rapid increase during the last 5 cycles tested. Fig. 2c shows that the FEC:TFEC containing cells had lower charge end-point capacity slippage rates than that of control cells and an increasing amount of PES lowered the charge end-point capacity slippage rates. Fig. 2d shows that the control cells and the FEC:TFEC cells have a capacity fade during the 600 h cycle-store experiments. Fig. 2e shows that the coulombic efficiency of the FEC:TFEC cells was higher than the control cells. Cells with 2%, 5% and 8% PES were also tested in the experiments described by Fig. 2. These results are not shown in Fig. 2 to avoid clutter but are included in summary graphs coming later.

Fig. 3a shows the open circuit voltage (OCV) versus time during 500 h of storage at 4.5 V for NMC442/graphite pouch cells with control electrolyte or with 1% or 3% PES in FEC:TFEC electrolyte at  $40 \pm 0.1$  °C. The voltage drop during storage indicates the occurrence of electrolyte oxidation at the surface of the positive



**Fig. 4.** The area-specific Nyquist plots (a, c, e) and Bode plots of (b, d, f) negative electrode symmetric cells (a,b), positive electrode symmetric cells (c, d) and full coin cells (e, f) made from pouch cells after the UHPC cycle/store experiments with electrolytes indicated. The data in panels a to d have been divided by two so that good visual comparisons according to eq. (1) can be made to the data in panel f. The real part of the impedance of the full cell calculated according to eq. (1) has been included in panel f.

electrode and has been shown to correlate well with charge endpoint capacity slippage [31]. Cells with larger charge endpoint capacity slippage rate during cycling normally have larger potential drops during storage and this correlation is clearly observed in Figs. 2c and 3a. Compared with control cells, the FEC:TFEC:PES containing cells show smaller potential drop and an increasing amount of PES led to better storage performance at 40.0 °C. Storage data was also collected for 2, 5 and 8% PES in FEC:TFEC, but that data has been omitted from Fig. 3 to avoid clutter. It will be presented in summary graphs later below.

Fig. 3b–d show the impedance spectra of NMC442/graphite pouch cells containing FEC:TFEC electrolyte with different amounts of PES after formation (Fig. 3b), after 500 h of storage at 4.5 V and 60 °C (Fig. 3c) and after UHPC cycling (Fig. 3d), respectively. The EIS measurements were made after cells were discharged to 3.80 V and cooled to 10. ± 0.1 °C. Charge transfer resistance ( $R_{ct}$ ) was calculated from the width of the semi-circle in the Nyquist representation of the electrochemical impedance spectra. In this work,  $R_{ct}$  includes the active particle-current collector contact resistance of both electrodes (small), the resistance to the transfer of  $Li^+$  from the electrolyte to the electrode through the solid electrolyte interface (SEI) of both electrodes, and the electron transfer to the active material of both electrodes [38]. Fig. 3b–d show that all cells with FEC:TFEC:PES electrolyte had much larger impedance than control cells and that the impedance increased as the amount of PES increased. During the storage or UHPC cycling experiments, all cells containing FEC:TFEC:PES showed a large impedance rise.

Fig. 4a, c and e show the area-specific Nyquist plots of negative (4a) and positive (4b) electrode symmetric cells as well as full coin cells (4e) containing control (1 M  $LiPF_6$  EC:EMC = 3:7) as well as 2% PES in FEC:TFEC electrolyte, respectively. Fig. 4b, d and f show the Bode plots of the real area-specific impedance as a function of frequency on a logarithmic axis for the same cells. The data in Fig. 4a–d have been divided by two for easy comparison to the full cell data since it has been previously shown that:

$$\frac{1}{2} Z_- + \frac{1}{2} Z_+ = Z_f, \quad (2)$$

where  $Z_-$ ,  $Z_+$  and  $Z_f$  are the impedances of the negative electrode symmetric cell, the positive electrode symmetric cell and the full cell, respectively [32]. These symmetric (or full) coin cells were made from the pouch cells after the UHPC cycle/store experiments. Some impedance spectra in Fig. 4 exhibit two semi-circles. This due to the double sided electrodes from the parent pouch cells which have poor conductivity to the cell hardware (cans, springs and spacers). This effect is not as obvious in the negative electrode symmetric cells (made from two graphite electrodes) since the graphite electrode has much better conductivity than the NMC electrode. Therefore, the high frequency semi-circle originates from the contact impedance and the lower-frequency semi-circle originates from  $R_{ct}$ . Fig. 4 shows that the control cell after UHPC cycling showed large positive electrode impedance and small negative electrode impedance. By contrast, cells containing 2% PES in FEC:TFEC electrolyte had large negative electrode impedance and

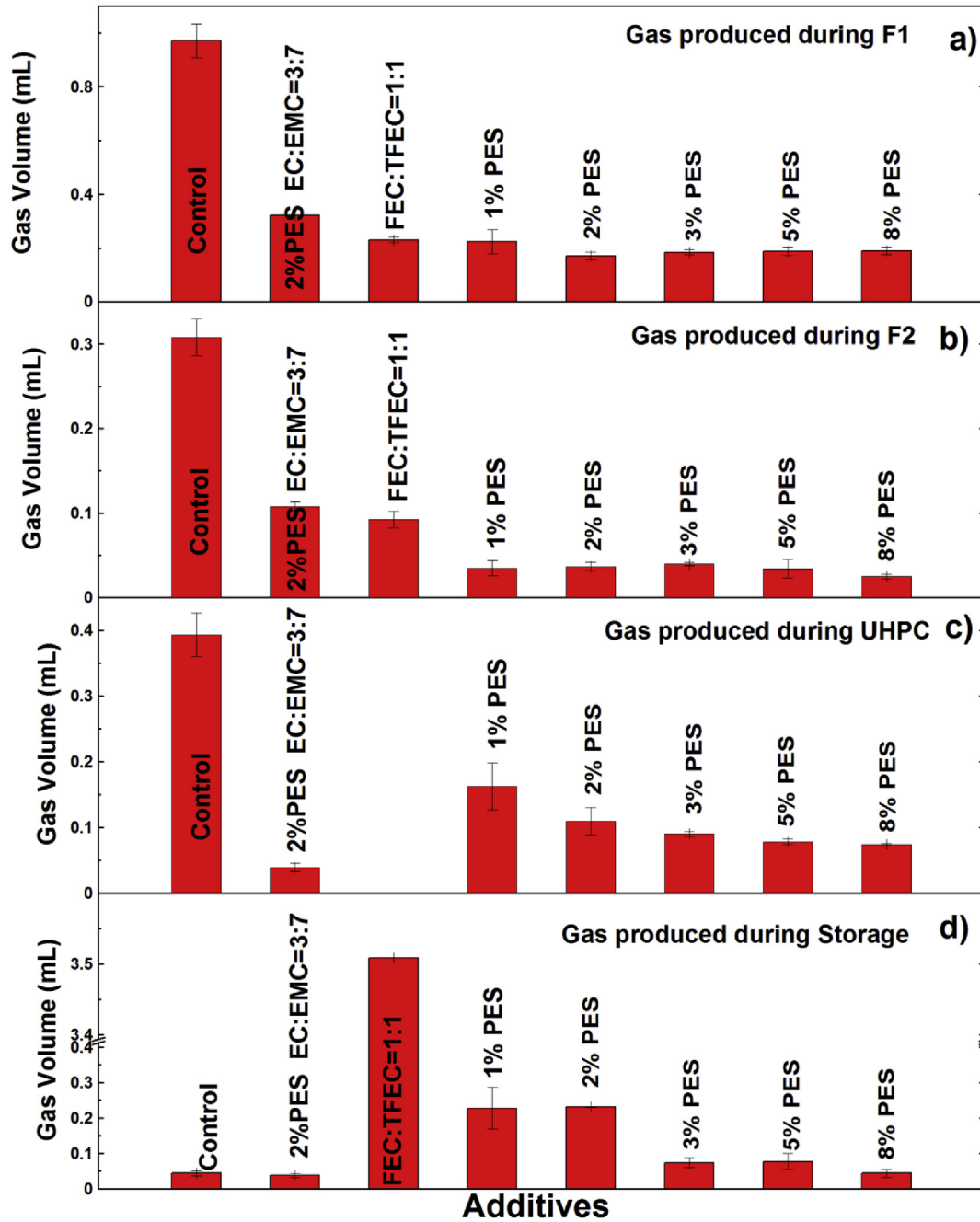
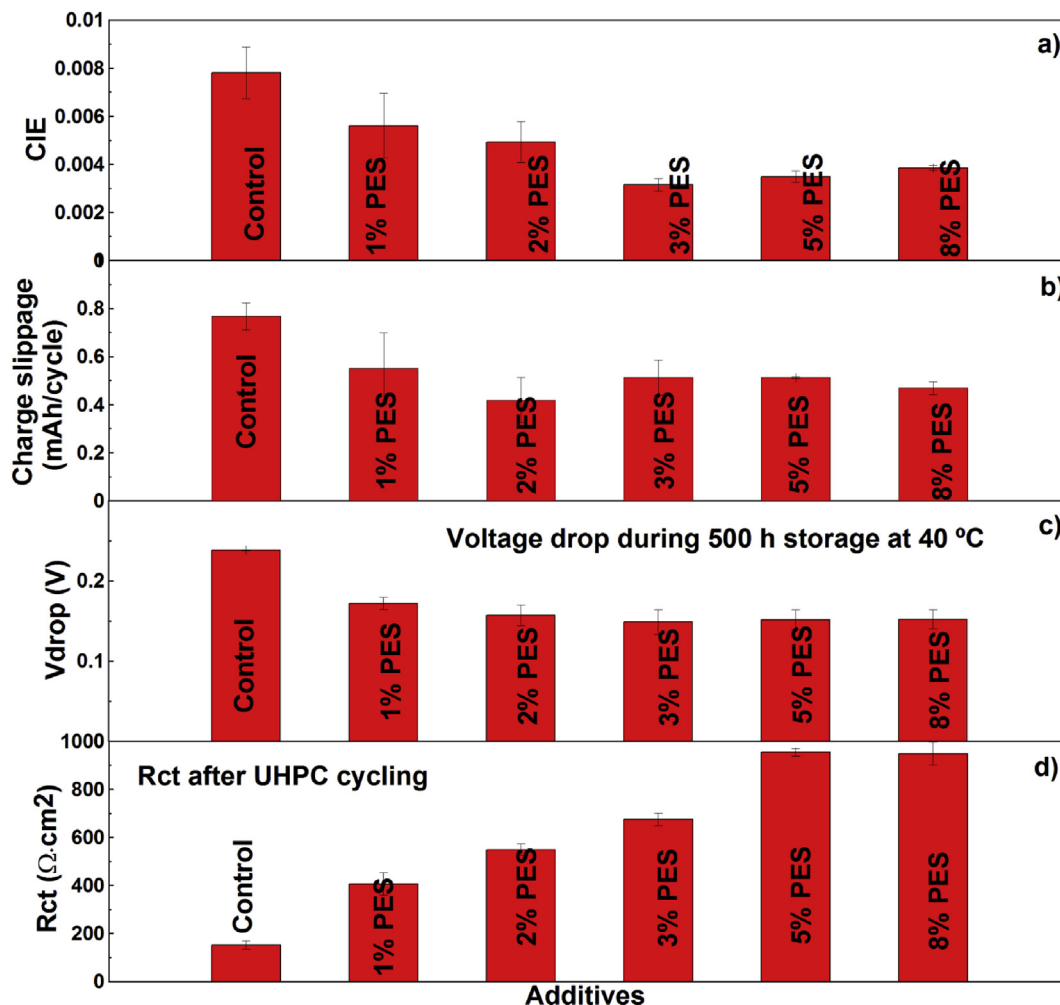


Fig. 5. Volume of gas evolved during: (a) formation step 1; (b) formation step 2; (c) the 500 h storage at  $40.0 \pm 0.1$  °C and (d) the 600 h UHPC cycle/store experiment at  $40.0 \pm 0.1$  °C.

small positive electrode impedance. Therefore, the high impedance of full cells with FEC:TFEC electrolyte is from the negative electrode (thick SEI film) and the beneficial effect of using FEC:TFEC electrolyte is mainly on the positive electrode side. A visual comparison of Fig. 4b, d and f suggests that if the data in 4b and 4d were added that the sum would match the data in Fig. 4f well as expected based on eq. (1). Fig. 4f shows the comparison between the predictions of eq. (1) and the full cell measured data, demonstrating good agreement. Some of the pouch cells containing PES in FEC:TFEC electrolyte were left at 3.8 V after UHPC cycling for 8 months. Then symmetric cells were made from those cells. Fig. S2 in the supplementary information shows that the positive electrode impedance of cells containing FEC:TFEC-based electrolyte is quite stable while the negative impedance decreases after 8 months. The reason

for the decrease in the negative electrode impedance is unknown.

Fig. 5a – 5d show the volume of gas produced in NMC442/graphite pouch cells with different amounts of PES in FEC:TFEC electrolyte during formation step 1, formation step 2, UHPC cycle/store at  $40.0 \pm 0.1$  °C and 500 h storage at  $40.0 \pm 0.1$  °C (4.5 V), all measured using the *ex-situ* Archimedes method. Each data point in Fig. 5 represents the average of two cells and the error bars are the standard deviation of the results. Fig. 5a and b show that the FEC:TFEC electrolyte produces less gas than control cells or control cells with 2% PES during both formation steps 1 and 2. Fig. 5c shows that cells containing FEC:TFEC:PES electrolyte produced less gas than control cells during UHPC cycling and that the volume of gas decreased with PES content. Fig. 5d shows that cells containing FEC:TFEC without PES produced a huge amount of gas during



**Fig. 6.** Summary of cycling and storage data collected in this study including: (a) CIE; (b) the charge endpoint capacity slippage; (c)  $V_{\text{drop}}$  during 500 h storage at 40 °C and 4.5 V (d)  $R_{\text{ct}}$  after UHPC cycling.

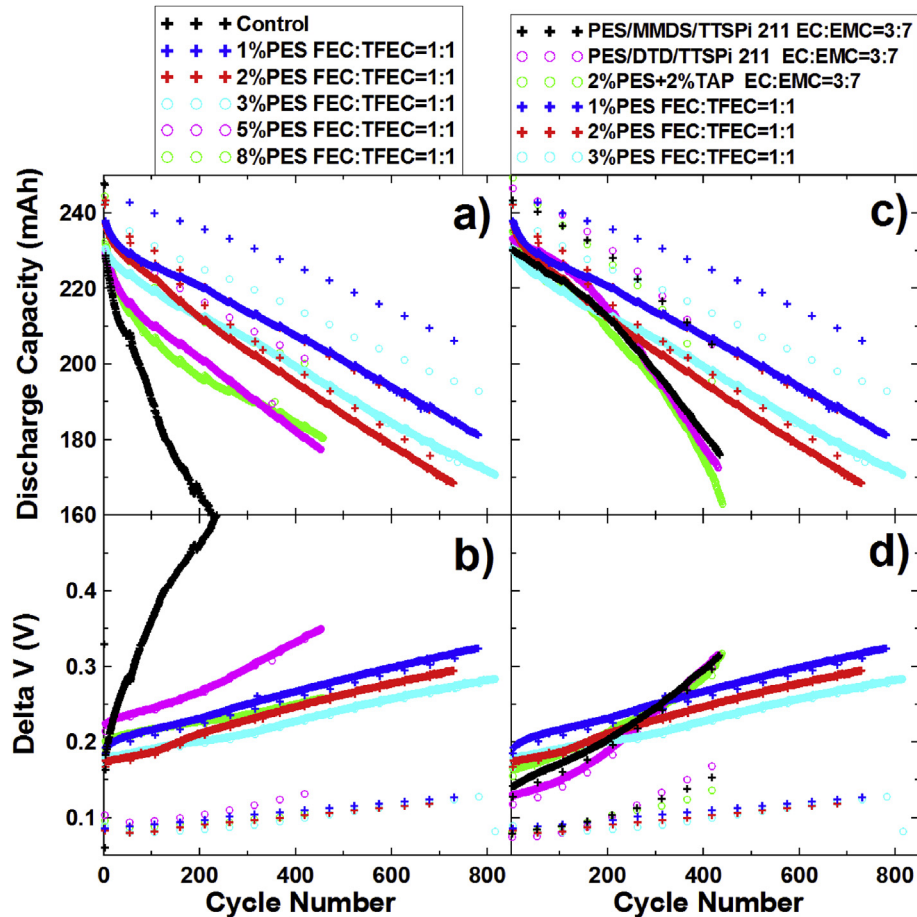
storage. Fig. 5d also shows that cells containing FEC:TFEC:PES electrolyte produced more gas than cells with control electrolyte or than cells with control electrolyte and 2% PES during the 500 h storage test. No gas data is available for cells with FEC:TFEC electrolyte with no PES after UHPC cycling (missing data in Fig. 5c).

Fig. 6a–d summarize the coulombic inefficiency (CIE), the charge endpoint capacity slippage during UHPC cycling, the voltage drop,  $V_{\text{drop}}$ , during 500 h storage at 4.5 V and 40 °C, and  $R_{\text{ct}}$  after UHPC cycling. The CIE was calculated from the CE by taking an average of the final three data points (cycles 13–15) collected on the UHPC while the charge endpoint capacity slippage was calculated from the slope of a best fit line to the final five points (cycles 11–15) of the charge endpoint capacity vs. cycle number curves. Fig. 6 shows that all the FEC:TFEC containing cells have lower CIE, smaller charge end capacity slippage rate, lower voltage drop during 500 h storage at 4.5 V and higher impedance than that of control cells. An increasing amount of PES (less than 3%) in FEC:TFEC electrolyte generally leads to lower CIE, smaller charge endpoint capacity slippage rate, lower voltage drop during 500 h storage at 4.5 V as well as lower gas evolution during UHPC cycling and storage tests (Fig. 5). However, when the PES content is higher than 3%, an increasing amount of PES has minimal effect on the cycling or storage performance. Therefore, high concentrations of PES (>3%) in FEC:TFEC electrolyte is not recommended.

Fig. 7a shows the capacity versus cycle number for NMC442/graphite pouch cells with different amounts of PES in FEC:TFEC electrolyte. Data for only one cell is available here because the other cells were used for the symmetric cell studies (Fig. 4). Fig. 7a shows the cells containing PES in FEC:TFEC electrolyte have much better capacity retention than that of cells with control electrolyte. Fig. 7b shows the difference between average charge and discharge potential ( $\Delta V$ ) vs. cycle number for the same cells. A smaller value of  $\Delta V$  means there is smaller polarization and thus smaller overall cell impedance [37]. Fig. 7b shows cells containing FEC:TFEC:PES electrolyte have more stable  $\Delta V$  than cells with control electrolyte. Fig. 7 shows cells containing FEC:TFEC:PES with PES contents greater than 3% have larger  $\Delta V$  and more rapid capacity fade, indicating that large amounts of PES are not useful.

In previous studies, “PES-211” [25] and tri-allyl phosphate (TAP) [39] were shown to be beneficial in suppressing impedance growth when NMC442/graphite cells were cycled up to and above 4.4 or 4.5 V. Compared with cells containing only 2% VC or 2% PES, cells with “PES-211” or 2% TAP had better capacity retention and less impedance growth during cycling to higher voltage. It is therefore important to compare the results from the cells containing FEC:TFEC:PES electrolyte with PES-211 or 2% PES + 2% TAP in 1 M LiPF<sub>6</sub> EC:EMC 3:7 electrolyte.

Fig. 7c and d compare the discharge capacity as well as  $\Delta V$



**Fig. 7.** NMC442/graphite pouch cells cycled with clamps at C/2.4 (100 mA) between 2.8 and 4.5 V at  $40 \pm 0.1$  °C with different concentrations of PES in FEC:TFEC electrolyte. (a) capacity and (b)  $\Delta V$ , both plotted vs cycle number. Panels c) and d) compare the PES:FEC:TFEC cell results to those for cells with EC:EMC-based electrolytes as indicated in the legend.

versus cycle number for NMC442/graphite pouch cells containing FEC:TFEC:PES electrolyte and “PES-211” or 2% PES + 2%TAP in EC:EMC 3:7 electrolyte. Fig. 7c and d shows the cells containing FEC:TFEC:PES electrolyte have much better capacity retention and less impedance growth during long-term cycling than the cells that containing “PES-211” or 2% PES + 2%TAP in EC:EMC electrolyte. The NMC442/graphite pouch cells with 1% PES in FEC:TFEC electrolyte could cycle 800 times to an upper cutoff of 4.5 V with less than 20% capacity loss, even at 40 °C which is very promising for the application in real devices.

Fig. 8 shows the charge transfer resistance,  $R_{ct}$ , as a function of potential measured every 5 cycles for cells with the indicated electrolytes. These cells were cycled aggressively at 40 °C on an automated cycling/EIS system and were held for 24 h at the top of charge (4.5 V) every cycle. The details of the cycling protocol used during the automated cycling/EIS procedure is shown in Fig. S3 (Supplementary Information). Fig. 8 shows the large impedance increase with both cycle number as well as voltage for cells with control electrolyte and for cells with 2% PES in EC:EMC 3:7. By contrast, the impedance of cells containing FEC:TFEC:PES electrolyte does not increase with potential which differs from the results for the EC:EMC based electrolytes shown here. However, although the impedance does not increase with potential for the FEC:T-FEC:PES cells, it does increase with cycle number. Recent work by Nelson et al. [40] [41] shows that NMC442/graphite cells with 2% PES + 2% DTD + 2% TTSPi in EC:EMC 3:7 can be charged to 4.45 V (not 4.5 V) with the same protocol as the FEC:TFEC:PES cells in

Fig. 8 and also show  $R_{ct}$  that does not increase with potential but does increase with cycling. This suggests that, with the right additive blends, the properties of EC:EMC electrolytes might closely match those of FEC:TFEC based systems.

Fig. S4 and S5a show the EIS data collected after long-term cycling for the same cells shown in Fig. 7. For cells containing control electrolyte, the impedance was measured when the cells had zero capacity and therefore is not very meaningful. Fig. S4 and S5a show that the impedance of cells containing PES:FEC:TFEC electrolyte decreases after long-term cycling compared to the EIS data after UHPC cycling shown in Fig. 6d. As the PES content in FEC:TFEC:PES electrolyte increases, the impedance of the cells after long-term cycling also increases which agrees with the data in Figs. 3 and 6d.

Fig. S5b shows the gas volume produced by the NMC442/graphite cells after the long-term cycling (Fig. 7) and automated cycling/EIS tests (Fig. 8) cycling (both tests were at 40 °C). During the long term cycling (Fig. 7), control cells produced about 0.9 mL gas. The cells containing FEC:TFEC with 1% PES produced 1.6 mL gas while the cells containing PES-211 in EC:EMC cells produced only about 0.11 mL gas. With an increasing amount of PES in FEC:TFEC electrolyte, the gas evolution decreased to about 0.15 mL of gas at 8% PES in FEC:TFEC. The reader is reminded that an increasing amount of PES increases the impedance and the capacity loss during cycling. Clearly a trade-off between gas production, impedance as well as capacity retention has to be considered.

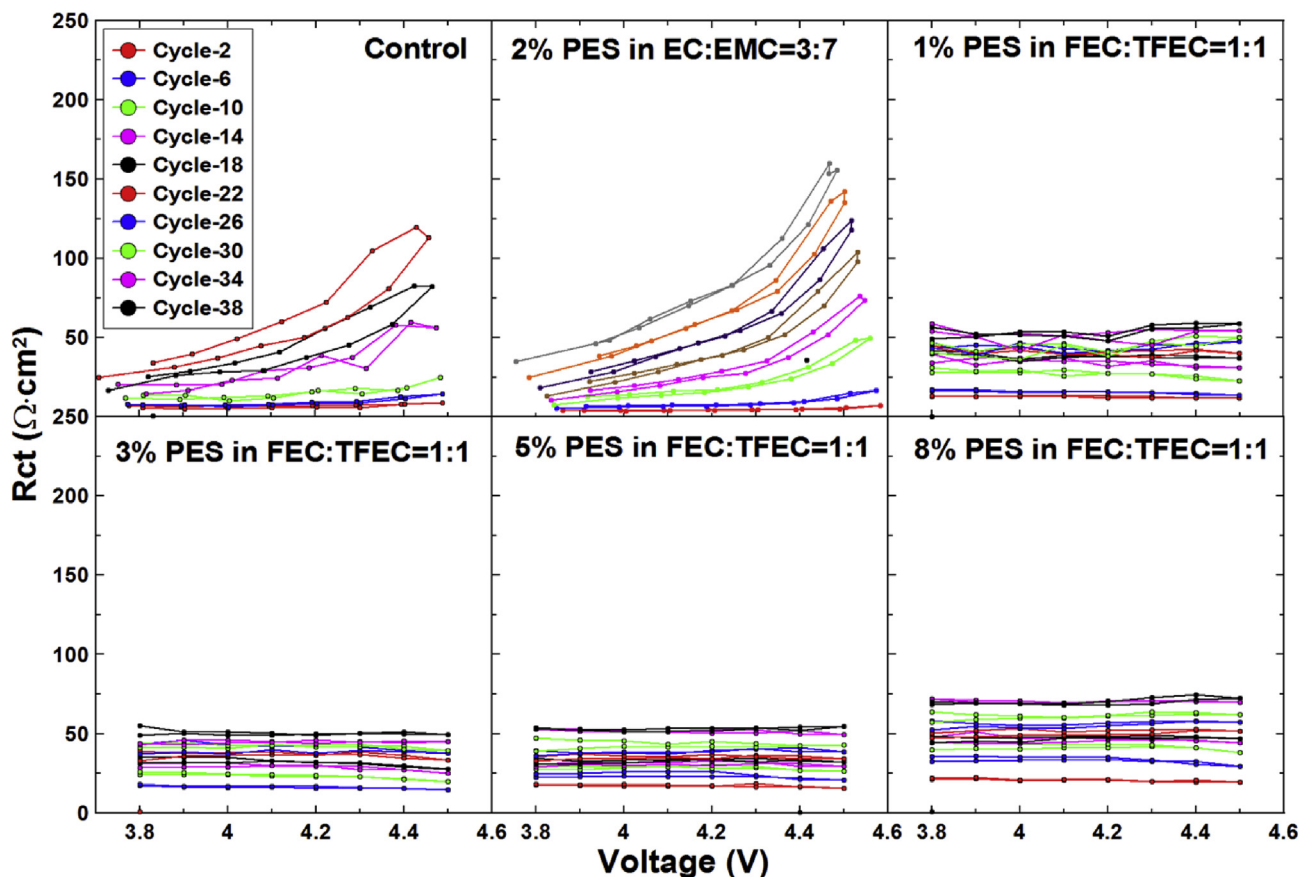


Fig. 8. The charge transfer resistance,  $R_{ct}$ , as a function of voltage measured every 5 cycles for cells containing PES in FEC:TFEC electrolyte. The cells were charged and discharged using the protocol shown in Fig. S3 (supplemental information) which had a 24 h hold at 4.5 V every cycle. The cells were tested at 40 °C.

#### 4. Summary and conclusions

FEC:TFEC-based fluorinated electrolytes containing different amounts of PES for high-voltage applications were studied in NMC442/graphite pouch-type Li-ion cells. The experimental results showed that without PES, cells containing FEC:TFEC electrolyte produced large amounts of gas during storage. PES acts as a gas reducer in both EC:EMC electrolyte and in FEC:TFEC electrolyte. Compared with state-of-the-art control electrolyte, cells containing PES:FEC:TFEC electrolyte showed much better long-term cycling and storage performance. The long-term cycling results showed that cells containing PES:FEC:TFEC electrolyte had better capacity retention than cells containing binary or ternary electrolyte additives in EC:EMC solvent that were reported in earlier publications [23,24]. Symmetric cell studies and EIS results suggested that the positive electrode in PES:FEC:TFEC electrolyte is relatively stable at potentials as high as 4.5 V. Nevertheless, the PES:FEC:TFEC electrolyte system has problems. Cells containing PES:FEC:TFEC electrolyte show very large negative electrode impedance which might limit high rate and low temperature applications. Gas evolution during long-term cycling and during charge/hold protocols is large even when gas reducing reagent, PES, is used as an additive. Further work is required to limit negative electrode impedance and limit gas generation.

#### Acknowledgment

The authors acknowledge the financial support of NSERC and 3M Canada under the auspices of the Industrial Research Chairs

program. The authors thank Dr. Jing Li of BASF for providing some of the solvents and salts used in this work. The authors thank Xiaodong Cao of HSC Corporation for supplying the TFEC used in this work.

#### Appendix A. Supplementary data

Supplementary data related to this article can be found at <http://dx.doi.org/10.1016/j.jpowsour.2015.12.132>.

#### References

- [1] B. Dunn, H. Kamath, J. Tarascon, *Science* 344 (2011) 929.
- [2] A. Kraytsberg, Y. Ein-Eli, *Adv. Energy Mater.* 2 (2012) 922.
- [3] S. Okada, S. Sawa, M. Egashira, J. Yamaki, M. Tabuchi, *J. Power Sources* 98 (2001) 430.
- [4] J. Wolfenstine, J. Allen, *J. Power Sources* 136 (2004) 150.
- [5] Z. Lu, D.D. MacNeil, J.R. Dahn, *Electrochem. Solid-State Lett.* 4 (2001) A200.
- [6] Q. Zhong, A. Bonaklapour, M. Zhang, J.R. Dahn, *J. Electrochem. Soc.* 144 (1997) 205.
- [7] J.R. Croy, D. Kim, M. Balasubramanian, K. Gallagher, S.-H. Kang, M.M. Thackeray, *J. Electrochem. Soc.* 159 (2012) A781.
- [8] K. Xu, *Chem. Rev.* 114 (2014) 11503.
- [9] X. Li, Y. Chen, C.C. Nguyen, M. Nie, B.L. Lucht, *J. Electrochem. Soc.* 161 (2014) A576.
- [10] K.-C. Möller, T. Hodal, W.K. Appel, M. Winter, J.O. Besenhard, *J. Power Sources* 97–98 (2001) 595.
- [11] J.-I. Yamaki, I. Yamazaki, M. Egashira, S. Okada, *J. Power Sources* 102 (2001) 288.
- [12] A. von Cresce, K. Xu, *J. Electrochem. Soc.* 158 (2011) A337.
- [13] M. Smart, B. Ratnakumar, V. Ryan-Mowrey, S. Surampudi, G.K. Prakash, J. Hu, I. Cheung, *J. Power Sources* 119–121 (2003) 359.
- [14] X. Chen, W.L. Holstein, WO2013033579 A1, 2013.
- [15] Z. Zhang, L. Hu, H. Wu, W. Weng, M. Koh, P.C. Redfern, L.A. Curtiss, K. Amine,

- Energy Environ. Sci. 6 (2013) 1806.
- [16] L. Hu, Z. Xue, K. Amine, Z. Zhang, J. Electrochem. Soc. 161 (2014) A1777.
- [17] L. Hu, Z. Zhang, K. Amine, Electrochem. Commun. 35 (2013) 76.
- [18] L. Hu, K. Amine, Z. Zhang, Electrochem. Commun. 44 (2014) 34.
- [19] Y. Wang, J. Jiang, J.R. Dahn, Electrochem. Commun. 9 (2007) 2534.
- [20] K. Lee, S. Myung, Y. Sun, Chem. Mater. 19 (2007) 2727.
- [21] J. Li, R. Petibon, S. Glazier, N. Sharma, W.K. Pang, V.K. Peterson, J.R. Dahn, Electrochim Acta 180 (2015) 234.
- [22] C.P. Aiken, J. Self, R. Petibon, X. Xia, J.M. Paulsen, J.R. Dahn, J. Electrochem. Soc. 162 (2015) A760.
- [23] J. Self, C.P. Aiken, R. Petibon, J.R. Dahn, J. Electrochem. Soc. 162 (2015) A796.
- [24] K.J. Nelson, G.L. Eon, A.T.B. Wright, L. Ma, J. Xia, J.R. Dahn, J. Electrochem. Soc. 162 (2015) A1046.
- [25] L. Ma, J. Xia, J.R. Dahn, J. Electrochem. Soc. 161 (2014) A2250.
- [26] R. Petibon, L. Ma, J.R. Dahn, Paper 292 Presented at the Electrochemical Society Fall Meeting, 2014. Cancun, Mexico, Oct.
- [27] T.M. Bond, J.C. Burns, D.A. Stevens, H.M. Dahn, J.R. Dahn, J. Electrochem. Soc. 160 (2013) A521.
- [28] N.N. Sinha, T.H. Marks, H.M. Dahn, A.J. Smith, J.C. Burns, D.J. Coyle, J.J. Dahn, J.R. Dahn, J. Electrochem. Soc. 159 (2012) A1672.
- [29] C.P. Aiken, J. Xia, D.Y. Wang, D.A. Stevens, S. Trussler, J.R. Dahn, J. Electrochem. Soc. 161 (2014) A1548.
- [30] J. Xia, J. Self, L. Ma, J.R. Dahn, J. Electrochem. Soc. 162 (2015) A1424.
- [31] N.N. Sinha, A.J. Smith, J.C. Burns, G. Jain, K.W. Eberman, E. Scott, J.P. Gardner, J.R. Dahn, J. Electrochem. Soc. 158 (2011) A1194.
- [32] R. Petibon, C.P. Aiken, N.N. Sinha, J.C. Burns, H. Ye, C.M. VanElzen, G. Jain, S. Trussler, J.R. Dahn, J. Electrochem. Soc. 160 (2013) A117.
- [33] M. Nie, J. Xia, J.R. Dahn, J. Electrochem. Soc. 162 (2015) A1186.
- [34] M. Nie, J. Xia, J.R. Dahn, J. Electrochem. Soc. 162 (2015) A1693.
- [35] J. Xia, L. Ma, C.P. Aiken, K.J. Nelson, L.P. Chen, J.R. Dahn, J. Electrochem. Soc. 161 (2014) A1634.
- [36] K.J. Nelson, J. Xia, J.R. Dahn, J. Electrochem. Soc. 161 (2014) A1884.
- [37] J.C. Burns, X. Xia, J.R. Dahn, J. Electrochem. Soc. 160 (2012) A383.
- [38] J. Xia, L. Ma, J.R. Dahn, J. Power Sources 287 (2015) 377.
- [39] J. Xia, L. Madec, L. Ma, L.D. Ellis, W. Qiu, K.J. Nelson, Z. Lu, J.R. Dahn, J. Power Sources 295 (2015) 203.
- [40] K.J. Nelson, D.W. Abarbanel, J. Xia, Z. Lu, J.R. Dahn, J. Electrochem. Soc. 163 (2016) A272.
- [41] K. Nelson, J.R. Dahn, ECS Conference on Electrochemical Energy Conversion & Storage with SOFC–XIV, July, 2015 abstract 457, Glasgow.